Report No. UMTA-VA-06-0065-79-1

LORAN POSITION DETERMINATION IN AN URBAN ENVIRONMENT: A COMPARISON OF THREE TECHNIQUES

OCTOBER 1979

Prepared for:

U.S. DEPARTMENT OF TRANSPORTATION
URBAN MASS TRANSPORTATION ADMINISTRATION
OFFICE OF TECHNOLOGY DEVELOPMENT AND DEPLOYMENT
Washington, D.C. 20590

Technical Report Documentation Page

1. Report No.	2. Government Accession No.	3. Recipient's Catalog No.
UMTA-VA-06-0065-79-1		

4. Title and Subtitle

Loran Position Determination In an Urban Environment: A Comparison of Three Techniques

5. Report Date
October 1979

6. Performing Organization Code

7. Author(s)
John S. Ludwick, Jr.

8. Performing Organization Report No.
MTR-79W00356

9. Performing Organization Name and Address
The MITRE Corporation, Metrek Division
1820 Dolley Madison Boulevard
McLean, Virginia 22102

10. Work Unit No. (TRAIS)

11. Contract or Grant No.
DOT-UT-90006

13. Type of Report and Period Covered

12. Sponsoring Agency Name and Address
U.S. Department of Transportation
Urban Mass Transportation Administration
400 7th Street, S.W
Washington, D.C. 20590

14. Sponsoring Agency Code

15. Supplementary Notes
Urban Systems Department
Project Number: 1242A

16. Abstract

As part of a multi-user Automatic Vehicle Monitoring system, relatively inexpensive Loran receivers will be used in a few vehicles to provide general location information over the entire 400 square mile Los Angeles basin. Three techniques to convert Loran time-difference-of-arrival information to latitude and longitude have been evaluated. All techniques gave approximately the same accuracy: mean and 95th percentile radial errors over a 30-square mile central area were approximately 650 feet and 1,700 feet, while over the entire area, the figures were approximately 1,500 and 2,800 feet. It appears that TD grid warpages in the Los Angeles area are large enough and not sufficiently regular to be compensated for by standard techniques.

17. Key Words	18. Distribution Statement
Loran Position Determination Determination Techniques Statistical Analysis Earth Models	Document is available to the U.S. public through the National Technical Information Service, Springfield, Virginia 22161

19. Security Classif. (of this report)	20. Security Classif. (of this page)	21. No. of Pages	22. Price
Unclassified	Unclassified		

Form DOT F 1700.7 (8-72) Reproduction of completed page authorized

ACKNOWLEDGMENT

Joe Howard, from MITRE Bedford, provided useful information on the present state of Loran algorithm development. He also provided initial copies of the algorithms tested.

METRIC CONVERSION FACTORS

Approximate Conversions to Metric Measures

Symbol	When You Know	Multiply by	To Find	Symbol
	LENGTH			
in	inches	2.5	centimeters	cm
ft	feet	30	centimeters	cm
yd	yards	0.9	meters	m
mi	miles	1.6	kilometers	km
	AREA			
in^2	square inches	6.5	square centimeters	cm^2
ft^2	square feet	0.09	square meters	m^2
yd^2	square yards	0.8	square meters	m^2
mi^2	square miles	2.6	square kilometers	km^2
	acres	0.4	hectares	ha
	MASS (weight)			
oz	ounces	28	grams	g
lb	pounds	0.45	kilograms	kg
	short tons (2000 lb)	0.9	tonnes	t
	VOLUME			
tsp	teaspoons	5	milliliters	ml
Tbsp	tablespoons	15	milliliters	ml
fl oz	fluid ounces	30	milliliters	ml
c	cups	0.24	liters	l
pt	pints	0.47	liters	l
qt	quarts	0.95	liters	l
gal	gallons	3.8	liters	l
ft^3	cubic feet	0.03	cubic meters	m^3
yd^3	cubic yards	0.76	cubic meters	m^3
	TEMPERATURE (exact)			
°F	Fahrenheit temperature	5/9 (after subtracting 32)	Celsius temperature	°C

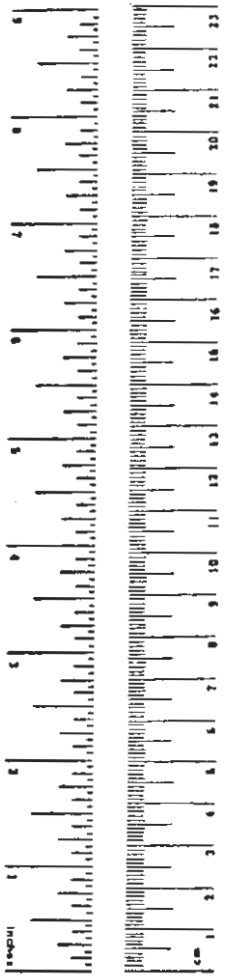

Approximate Conversions from Metric Measures

Symbol	When You Know	Multiply by	To Find	Symbol
	LENGTH			
mm	millimeters	0.04	inches	in
cm	centimeters	0.4	inches	in
m	meters	3.3	feet	ft
m	meters	1.1	yards	yd
km	kilometers	0.6	miles	mi
	AREA			
cm^2	square centimeters	0.16	square inches	in^2
m^2	square meters	1.2	square yards	yd^2
km^2	square kilometers	0.4	square miles	mi^2
ha	hectares (10,000 m^2)	2.5	acres	
	MASS (weight)			
g	grams	0.035	ounces	oz
kg	kilograms	2.2	pounds	lb
t	tonnes (1000 kg)	1.1	short tons	
	VOLUME			
ml	milliliters	0.03	fluid ounces	fl oz
l	liters	2.1	pints	pt
l	liters	1.06	quarts	qt
l	liters	0.26	gallons	gal
m^3	cubic meters	35	cubic feet	ft^3
m^3	cubic meters	1.3	cubic yards	yd^3
	TEMPERATURE (exact)			
°C	Celsius temperature	9/5 (then add 32)	Fahrenheit temperature	°F

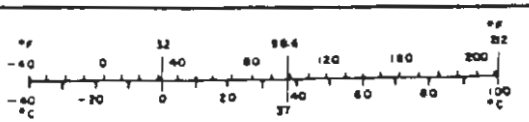

TABLE OF CONTENTS

LIST OF ILLUSTRATIONS

LIST OF TABLES

1. INTRODUCTION

The Urban Mass Transportation Administration (UMTA) and the Transportation Systems Center (TSC) are developing a multi-user Automatic Vehicle Monitoring (AVM) System to be deployed in a demonstration in Los Angeles. The basic fixed route location subsystem (for buses) utilizes low-power, high frequency "signposts" at intervals along the routes covered. Signposts also will be installed throughout a portion of the CBD, including the high rise area, at a density high enough to provide sufficient accuracy for random route vehicles in this area. In addition, a number of vehicles will be instrumented with a hybrid location subsystem, also including a Loran-C receiver and differential odometer, for operation over the entire 400 square miles of the Los Angeles basin.

Although the characteristics of Loran in seaborn application is well known, its use in land mobile applications, and especially in urban areas, is still in an exploratory stage. Loran-C was used by Teledyne during a test of candidate AVM technologies in Philadelphia; however, there were many parts of the city where the signal was inadequate for accurate position determination, and signpost augmentation was required for system operation.[1,2] The West Coast Loran chain, only recently operational, gave promise of providing a high quality signal in the demonstration area.

This report documents the evaluation of three commonly used techniques for conversion of Loran time-difference-of-arrival measurements to position estimates. The techniques varied in complexity; the comparison was designed to determine whether one particular technique was substantially superior with respect to accuracy, performance, and costs to the others. The analysis also attempts to ascertain which technique, if any, might be appropriate for a non-signpost random route application.

Even if the more complex techniques could provide better accuracy than the simpler ones (which has not been demonstrated), the incremental accuracy improvement might not justify the increased processing, which could only be performed at the central site.

The three basic types of algorithms tested were: an empirical regression technique using best-fit equations to fit measured time differences (TDs) to locations; a theoretical technique which uses a geometric earth model and a radio wave propagation model to determine location based on travel times from the known transmitters; and a combination technique which computes the position theoretically, then provides an empirical correction based on the relative position within the region calibrated. Data measured in the demonstration area in Los Angeles were used to determine the required coefficients which were then then used with a second set of data to evaluate the accuracy of each technique. A variety of graphical and statistical techniques were used to analyze the results. Processing time and core requirements were also measured for each method.

All techniques gave approximately the same accuracy; mean and 95th percentile errors over a 30 square mile area including the CBD were approximately 650 feet and 1,700 feet respectively, while for the entire 400 square mile area, the figures were approximately 1,500 feet and 2,800 feet. Comparative storage requirements for all methods were approximately the same, while the regression technique was approximately eight times faster than the combination method.

Plots of the predicted position versus actual position showed the predictions of all three methods at most points to be relatively near each other. This seems to indicate that the large TD warpages, if not actually random, are not sufficiently regular to be compensated for by standard techniques. The plots, overlaid on Geological Survey maps, did reveal a number of large errors near railroad tracks although other points seemingly similarly located did not show such errors.

2. LORAN THEORY AND OPERATION

The Loran (from Long Range Navigation) technique utilizes a network of transmitters at known locations, transmitting accurately synchronized pulse trains. Based on the difference in time of arrival of signals from the "master" and a "slave" transmitter at a receiver site (Figure 1), a hyperbolic line of position is defined on the surface of the earth. A second set of time differences between the master and a second slave defines another hyperbolic line of position whose intersection with the first line determine the location of the receiver (Figure 2).

Loran-C has been in general use for 15 years, with transmitter chains generally being established to provide coverage of coastal confluence areas. (There is also Loran-A, developed during the Second World War, which is less accurate and has a shorter range; and Loran-D, a lower power system intended for tactical military use.) Initially, the equipment required to locate vehicles using Loran was expensive, or large, or required time-consuming manual methods. Trade-offs could be made among these factors, depending upon the space and response time constraints, for shipborne or airborne use; in any case, cost was relatively small compared to the total cost of the vehicle. Use of such equipment for land vehicles would not have been feasible.

The advent of microcircuit technology has reduced the size and cost of receivers, while providing increasingly more sophisticated processing internal to the unit. The parameters of Loran receivers now make their use feasible in land mobile applications. However, there is no large body of data available to indicate the performance of such equipment in an urban environment. Closely controlled Loran tests have been performed in Philadelphia but the accuracy and coverage attained were inadequate for transit use. It was predicted that the newly operational West Coast chain would provide much better results in the Los Angeles area. Some of the problems affecting Loran in terrestrial, and especially urban use, are discussed below.

Loran-C, in order to provide a reliable and stable transmission path between transmitter and receiver, relies upon the ground wave propagation mode--that is, the signal path that travels along the surface of the earth as opposed to a signal path that reflects off the ionosphere, whose height, affecting the total signal travel time, can vary substantially. As attenuation of the ground wave signal increases rapidly with frequency, a low frequency, 100 KHz, was selected for Loran-C. Natural noise levels are high at this frequency, and today's automatic receivers use time domain sampling with progressively narrow windows to locate the proper pulse groups, then the proper cycle within each pulse.

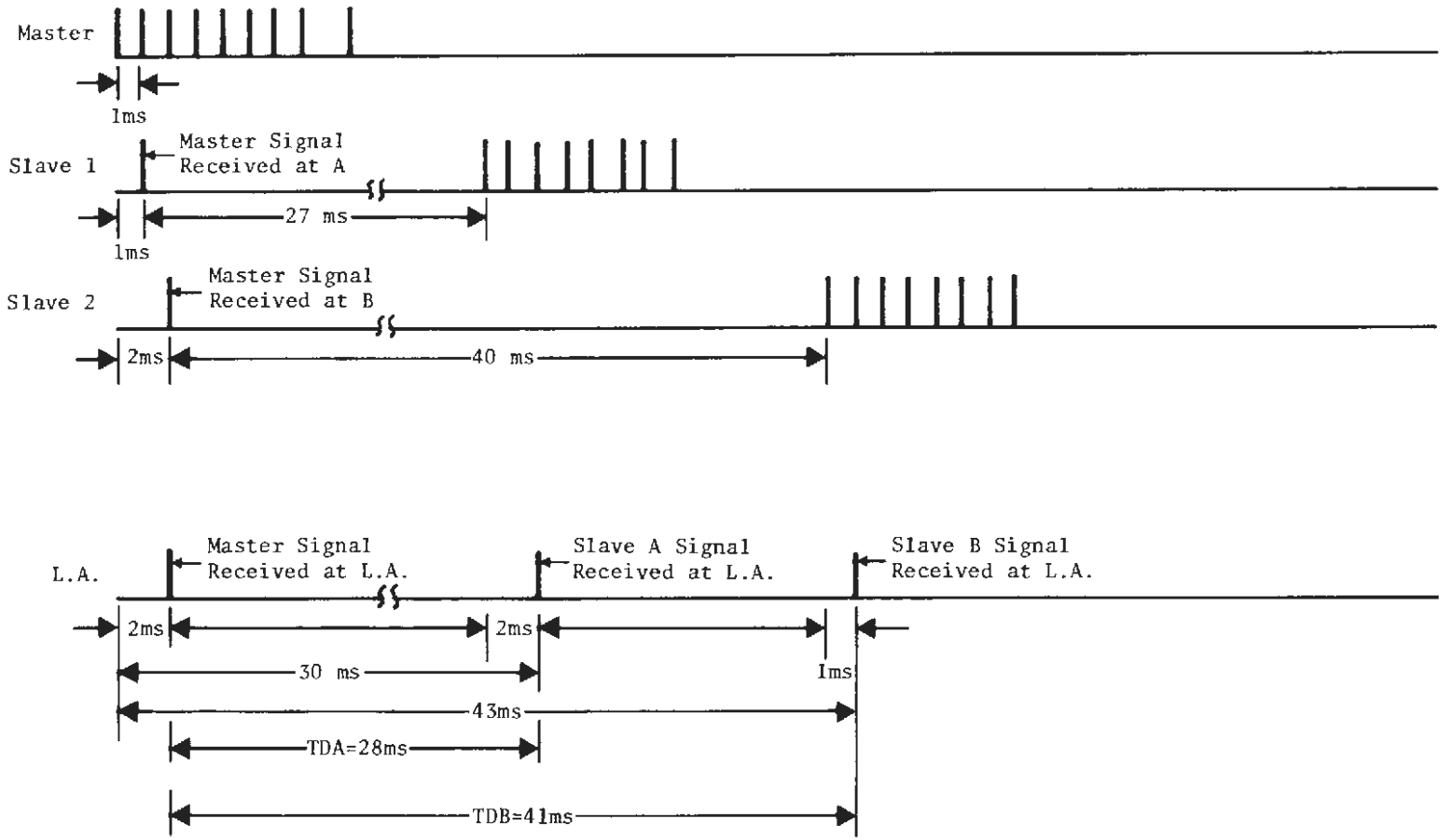

FIGURE 1
LORAN TIMING IN LOS ANGELES AREA

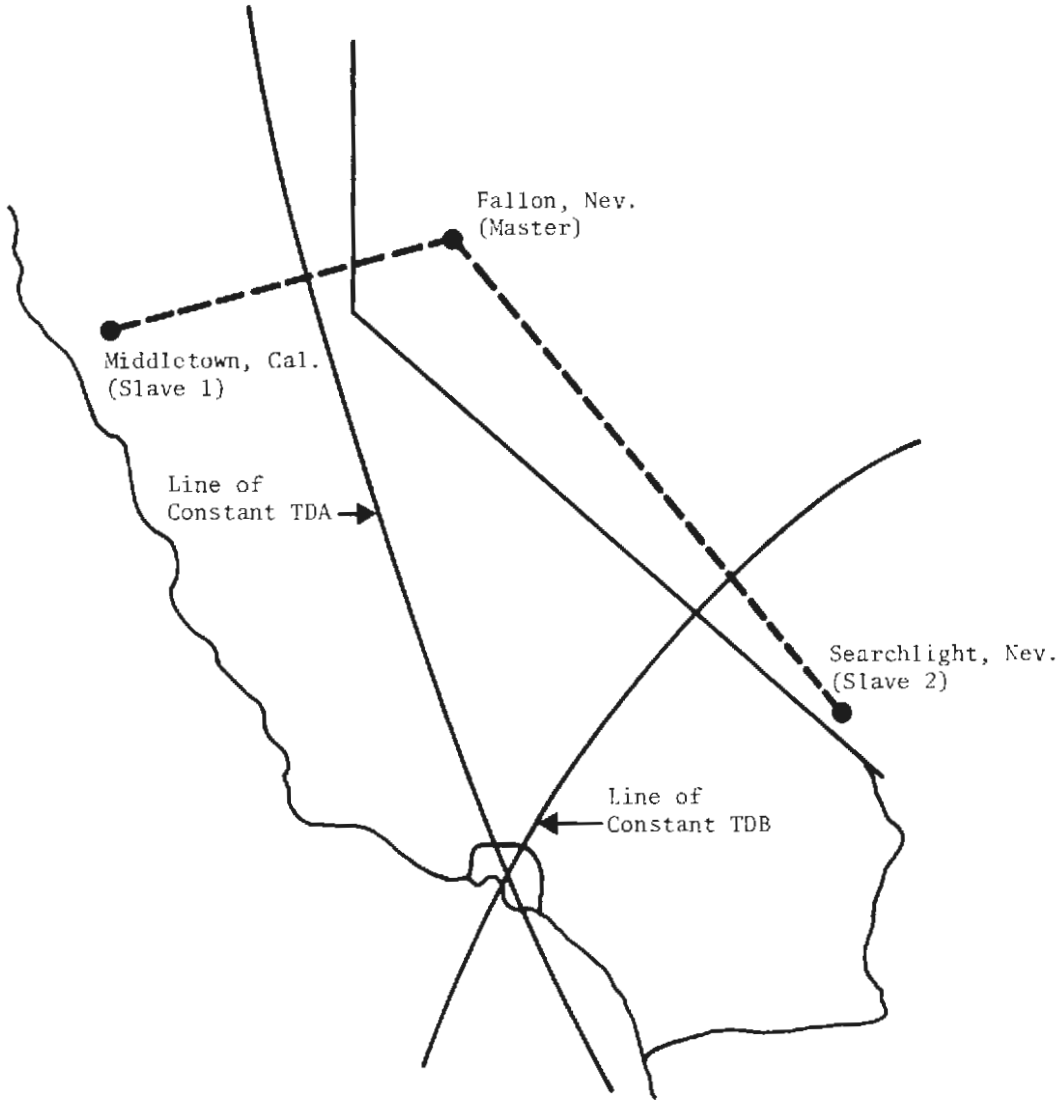

FIGURE 2
HYPERBOLIC TIME-DIFFERENCE GEOMETRY IN LOS ANGELES AREA

The speed with which this acquisition process converges on the proper point depends on the pulse group rate as well as the signal-to-noise ratio. One consequence of using a low transmission frequency is that the rate at which pulses can be sent is also limited. As a result, acquisition, or reacquisition after a signal is lost, takes from one to five minutes. Reacquisition is necessary when a signal level becomes too low, or when noise becomes too high for a period of time long enough that the receiver cannot adequately predict relative timing of the pulse train.

It was originally anticipated that the Los Angeles area would enjoy good Loran signal reception, as the farthest transmitter is only 400 miles away. However, during the collection of calibration point data, it was determined that the signal level of the master, which affects the computation of both TDs, was substantially lower than that of the two slaves. In addition, in many areas, high noise, evidently caused by increasing use of SCR controllers, was transmitted along power lines.[3] Carrier current signaling by utilities over transmission lines and inductive loop traffic detectors using frequencies within the Loran receiver bandpass, also resulted in severe interference.

In addition to signal and noise problems, the variation of ground conductivity between the transmitters and the receiver affects the propagation velocity of the signal. If the composition of the earth crossed by the signal between a transmitter and a receiver in different parts of the reception area changes substantially, a warpage of the lines of constant TD results. (As the conductivity of salt water is, for all practical purposes, constant, this problem is rarely encountered in shipboard use.) Other grid warpages can occur in the vicinity of long radiators, such as railroad tracks or power lines; high rise areas can also cause decreased signal and increased noise.

As the measurement to determine TDs is taken from a specific cycle of the 100 KHz pulsed signal, signal or noise problems, which are not sufficiently serious to cause loss of track, or rapid grid warpages can cause the incorrect cycle to be chosen, resulting in an error of ten microseconds or some multiple of it. As a ten microsecond change in the Los Angeles area corresponds to a position change of two to four miles, reasonability checks can be used to discriminate such cycle slip errors.

Obviously, algorithms to determine coordinate location based on TDs cannot compensate for lack of signal. (Other techniques <u>can</u> be used to extrapolate a probability contour based on the last received point, direction and speed of travel and route and schedule data.) However, some TD to X,Y conversion methods do attempt to account for the TD grid warpages existing in an urban area. The methods examined are discussed in the next section.

3. LORAN POSITION DETERMINATION TECHNIQUES

The techniques tested fall into three classes: a completely empirical curve fitting, or regression, technique; a theoretical, or iterative geometrical technique; and a technique that combines the theoretical and regression methods. The regression technique tested was developed by Teledyne[4] and used by them during the Philadelphia test; the theoretical technique used is described in Reference 5; and the combination technique is the method used in the AN/ARN-101 Loran receiver.[6]

3.1 Empirical

In the empirical approach a functional relation between two sets of measured data is derived. In this application, the data are time differences (TDs) and location. The locations can be expressed in nearly any coordinate system--longitude and latitude are used here, but relative position on a CRT is equally valid. It is assumed that there is some actual relationship between the data measured at the calibration points that can be approximated by a series of functions, the coefficients of which are determined from the measured data. Here the functions are powers of longitude and latitude (actually their difference from a reference position) and the technique is polynomial regression. Powers up to the fifth order can be handled by the program as it exists; an example of a third order relationship is:

$$x=a_1 T_A+ a_2 T_B+ a_3 T_A^2 + a_4 T_A T_B+ a_5 T_B^2+ a_6 T_A^3+ a_7 T_A^2 T_B+ a_8 T_A T_B^2+ a_9 T_B^3$$

$$y=b_1 T_A+ b_2 T_B+ b_3 T_A^2+ b_4 T_A T_B+ b_5 T_B^2+ b_6 T_A^3+ b_7 T_A^2 T_B+ b_8 T_A T_B^2+ b_9 T_B^3$$

Where, $T_A=TDA_{measured}-TDA_{reference}$; similarly for T_B.

Standard least-square techniques are used to determine the best fit coefficients (the a's and b's), as described in Appendix A. The program generating the coefficients is composed of 12 Fortran IV subroutines consisting of approximately 600 statements. If there actually is a functional relationship between the measured variables of the same form as used in the regression, the fit should be very good. As lines of constant TD are known to be hyperbolas, a second order polynomial should suffice. However, as it is known that there are TD distortions in urban areas, higher order polynomials may give better fits. Also, if it is assumed that there may be anomalies that affect all measurements in a given area, breaking the area up into a number of sectors each with its own empirically determined set of coefficients may improve overall accuracy.

The Teledyne program allows one to specify which data points are to be used to generate coefficients for different sectors. The original Teledyne position determination algorithm chose which set of sector coefficients to use by selecting the sector whose reference TD pair was closest, in an RMS sense, to the data point. During model evaluation, when multiple sectors were used, it was noted that a few points had very large errors, a condition that was traced to a point being assigned to a sector where, at least visually, it didn't belong. The reason is illustrated in Figure 3. The Loran transmitter-receiver geometry is such that a point closer in the TD domain to the sector reference point could actually be more distant in distance. The program was modified, using the following equations which give the gradient relationship between TDs and XYs, to assure that a point was used with the regression coefficients of the nearest sector.

$$\begin{bmatrix} dx \\ dy \end{bmatrix} = \frac{C_p}{\Delta} \begin{bmatrix} A & B \\ C & D \end{bmatrix} \begin{bmatrix} dTDA \\ dTDB \end{bmatrix}$$

Where $A = \cos x_M - \cos x_B$

$B = \cos x_A - \cos x_M$

$C = \sin x_B - \sin x_A$

$D = \sin x_M - \sin x_A$

$\Delta = AD - BC$

$dTDA = TDA_{computed} - TDA_{actual}$ (nanoseconds)

x_A = bearing from reference point to slave A, etc.

dx = change in East-West position (i.e., longitude change)

dy = change in North-South position (i.e., latitude change)

C_p = .98323886 feet/nanosecond

Using the West Coast Loran chain in the Los Angeles area, this results in:

$dx = 1.2\ dTDA - 0.4\ dTDB$

$dy = 2.0\ dTDA + 1.0\ dTDB$

TDA: Time difference of arrival of signals from Master and Slave 1.

TDB: Similarly, for Master and Slave 2.

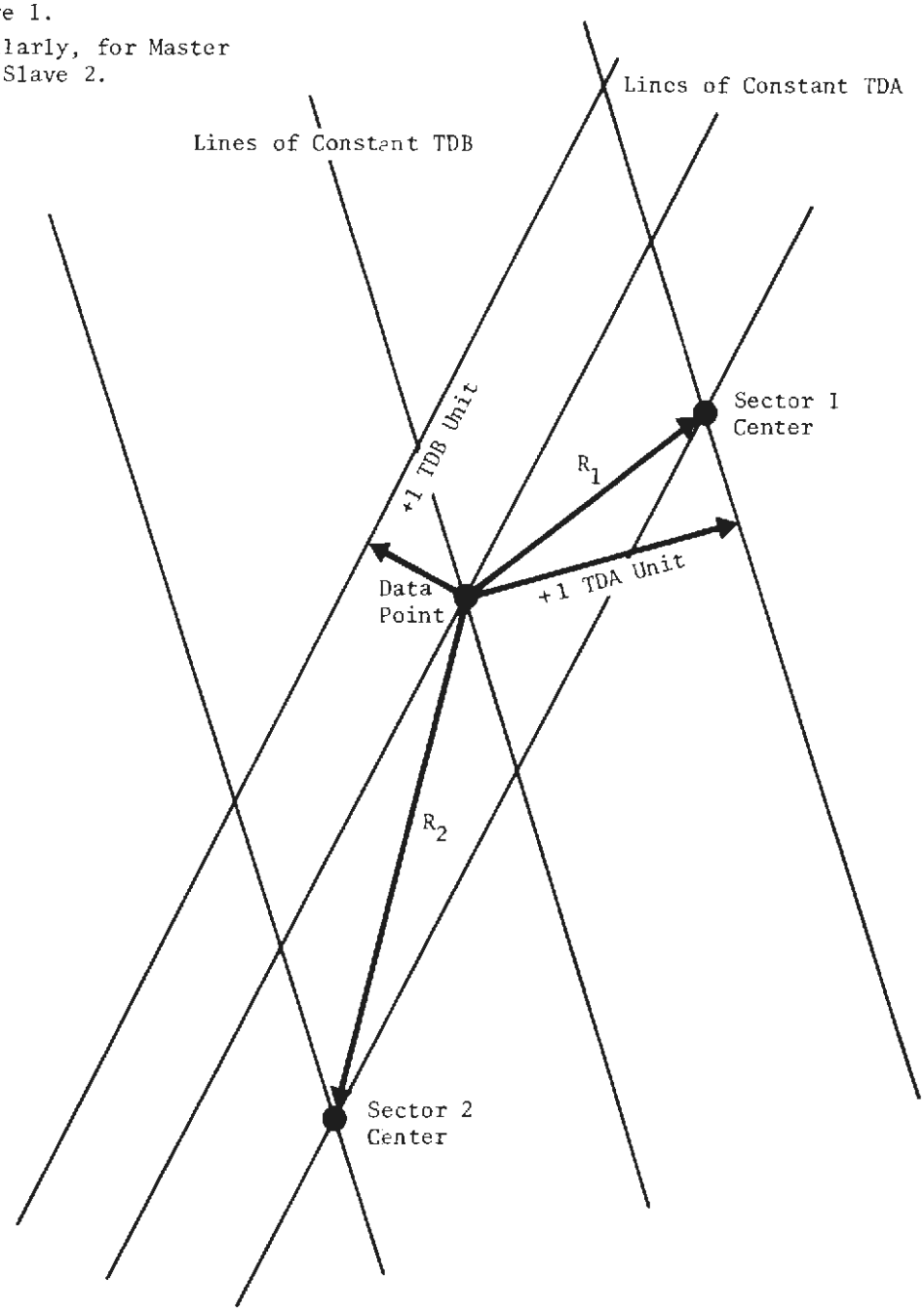

FIGURE 3
NEAREST SECTOR AS MEASURED BY TDs MAY NOT BE NEAREST IN DISTANCE

The regression technique is unequalled in speed of computation, as received TDs are just "plugged into" an equation, the output of which is the desired location. Coefficients for the equations have to be stored, however--up to 30 per sector for a fifth order regression, and a certain amount of computer time is required to chose the propser sector. Also, as the coefficients were chosen to fit points within a certain area, TDs from points outside that area may result in large errors.

3.2 Theoretical

The second major technique is here called theoretical because it uses an earth model and a propagation model to compute signal travel times between the known transmitter sites and the assumed receiver site. Figure 4 illustrates the technique. The amount by which the computed TDs differ from the received TDs is used with the gradient equation previously discussed to improve the estimate of the assumed receiver position. This process is repeated until successive position estimates are close enough (ten feet in the program tested) or some iteration threshold (here, nine) is exceeded. Signal travel times are composed of a primary component, the time taken for light to travel in air between the transmitter and the assumed receiver position, and a secondary component, accounting for an additional delay caused by transmission over finitely conducting earth. Strictly speaking, the technique as tested did have an empirical aspect. Although the conductivities along the transmission paths can be determined approximately by knowing the type of soil along the path (and what proportion of the path is over sea water), and in fact can be determined quite precisely if detailed geological data is available, final determination of conductivities was accomplished by trial and error modifications until computed TDs best approximated measured TDs at calibration points.

Three types of earth models were used in different tests of the theoretical technique: two forms of flat earth models with corrections, and a more complex precision earth model. The equations for the various models are given in Appendix B. The simplest flat earth model uses plane geometry to determine range and bearing between points, with the following corrections: the North-South range component is computed by decreasing the equatorial radius by a flattening constant and the East-West range component uses the equatorial radius multiplied by the cosine of the average of the latitudes of the two points. The latter correction helps account for the convergence of longitude lines as they approach the poles. Bearing is then determined from the arctangent of the range components. The more complex flat earth model includes, in the range computations, higher powers of the flattening constant multiplied by the $\sin^2$ of the reference position latitude. A latitude-dependent bearing

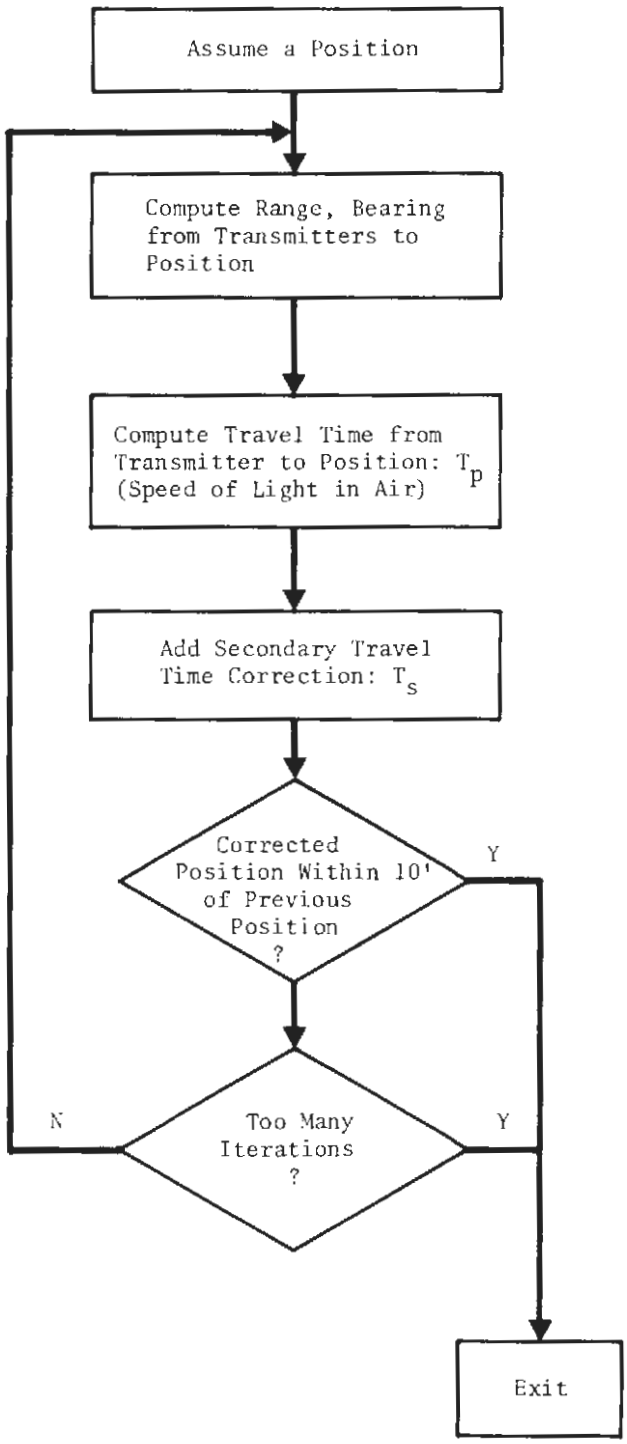

FIGURE 4
ITERATIVE GEOMETRY TECHNIQUE USED BY THEORETICAL AND COMBINATION METHODS

correction is also used. The precision earth model used was taken from the combination method and uses much more complex functions of four spheroidal constants. To determine the accuracy of the various earth models, surveyed ranges and bearings between the various West Coast transmitter sites were obtained from the Coast Guard and compared with figures predicted in Table 1. It can be seen that each level of added complexity does substantially improve the range and bearing accuracy. This does not necessarily imply a corresponding improvement in Loran position determination accuracy, as the process of choosing the conductivity values compensates for these biases. It does, however, affect the number of iterations required for the process to converge; using typical Los Angeles data points, three iterations were required using the simplest flat earth model, two each with the more complex flat earth model and the precision earth model.

As this technique is iterative, it is more time consuming than the regression technique. It does have the advantage of being relatively accurate over areas outside of where it was calibrated. (Changes in distance of the signal path are handled by the earth model, but large changes in the composition of the earth crossed by signals cannot be.)

3.3 Combination

The third technique combines aspects of the theoretical and empirical techniques. The primary phase is computed as described for the theoretical method, using the precision earth model. The secondary phase contribution, however, is calculated based on coefficients previously computed from calibration point data. Figure 5 shows the flow chart of the secondary phase computation. Once the total signal travel times are computed, the iterative process of determining location is the same as for the theoretical techniques.

The program to determine the coefficients first forms an effective impedance map for each transmitter over the area of interest (that is, a map of how much the signal is impeded at the calibration points) then fits a set of functions to each impedance map using least squares techniques. The program, comprising 35 subroutines and 3,000 statements, was originally written in Fortran for CDC equipment, and was converted by the author to run on IBM computers. This required converting all variables and functions to double precision values (CDC's standard word length is 60 bits, while IBM's is 32 bits), which in turn required writing some double precision functions not supplied with the Fortran G1 compiler available at Metrek. Also, a number

TABLE 1 MAXIMUM RANGE AND BEARING ERRORS OF EARTH MODELS

	Range (Ft.)	Bearing (Deg.)
Flat Earth + Mid-Latitude Correction	- 2,000	± 2.40
Flat Earth + Extensive Corrections	+ 800	± 0.15
Precision Earth	± 30	± 0.06

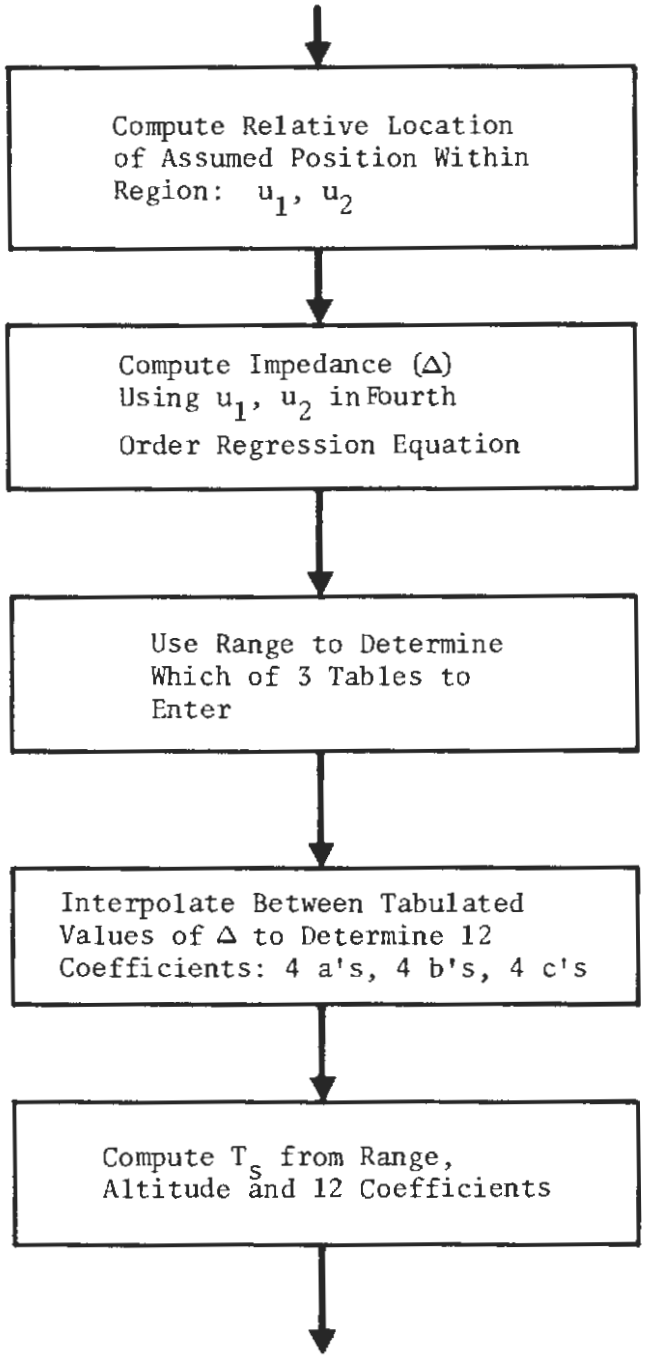

FIGURE 5
DETERMINATION OF SECONDARY PHASE CORRECTION FOR COMBINATION METHOD

of Function subprograms were changed to Subroutines, as Fortran does not permit the specification of double precision complex Functions. Even then, the results were not identical, but the maximum theoretical radial difference in Los Angeles would be only 15 feet.

It may be questioned whether there is any theoretical justification for believing that a given order or regression applied in the combination technique should provide any more accuracy than the same order of regression applied in the empirical technique. Intuitively, it does seem that by fitting functions to each of the three transmitters and using the results only to correct for differences from primary travel times separately computed, more flexibility is available then when a direct TD to XY curve fit is used. However, there are only two independent pieces of information available for use by the either technique, the two TDs, and using them in three equations instead of two, is no guarantee of improved performance. Essentially the question is whether an impedance function (perturbed by the existing noise) is better than the direct conversion of TD's (perturbed by the existing noise) to XY. At least when applied to the Los Angeles environment and the types of TD perturbations encountered there, the end results seem to indicate little difference between the two techniques.

4. ANALYSIS TECHNIQUES

The analysis of the various Loran position determination algorithms was directed at determining relative measures of performance and cost for each technique. Performance relates to the accuracy of the technique; mainly represented here by the mean, standard deviation and 95th percentile accuracy. Cost relates to the processing time and storage requirements of a given technique, as a simple enough technique could be performed on-board a vehicle. In addition to relieving the central processor of a large amount of routine processing, an on-board processor could perform continuous smoothing and reasonability checks using data that could not be available to the central computer.

The analysis technique was designed to simulate the manner in which the algorithms would be used. A data base of 800 points in a 30 square mile area including the CBD (the "central" area) and 100 points over a 400 square mile area including most of the Los Angeles basin (the "wide" area) was collected in July 1978 by Teledyne during an earlier phase of the project. Figure 6 shows these areas. The raw data required a substantial amount of effort to convert it to a useful form. Separate analyses were made of the central and wide area data. Every tenth data point was selected from the random route area, and every other point from the wide area, to be used to generate the required coefficients or conductivities required by the different techniques. A second sample, the same size as the first, was then chosen to simulate the system use. The previously determined coefficients were used to predict the locations at these points, based on the received TDs, and the predicted and actual locations were compared.

The raw data was in the form of one data sheet for each measurement point, including three sets of TDAs and TDBs, the location of the point with respect to the nearest intersection and comments (e.g., "near power line", "lost track", etc.). After sample data points were selected, longitude and latitude was then determined by plotting the locations on 7 1/2 minute Geological Survey maps. For one not familiar with every street in Los Angeles, this required first consulting a detailed city map, then locating the corresponding points on the larger maps. To assist in determining at least the approximate location, a plotter program using the gradient relation previously discussed, along with a pair of TDs whose approximate position was known, was used to plot the relative positions of all the other TDs to the same scale as the maps used. The plot could then be overlaid on the map to determine an approximate area on which to concentrate. Once the points were located, their longitude and latitude were determined by using a pair of ruler scales also generated by the plotter, directly in decimal degrees.

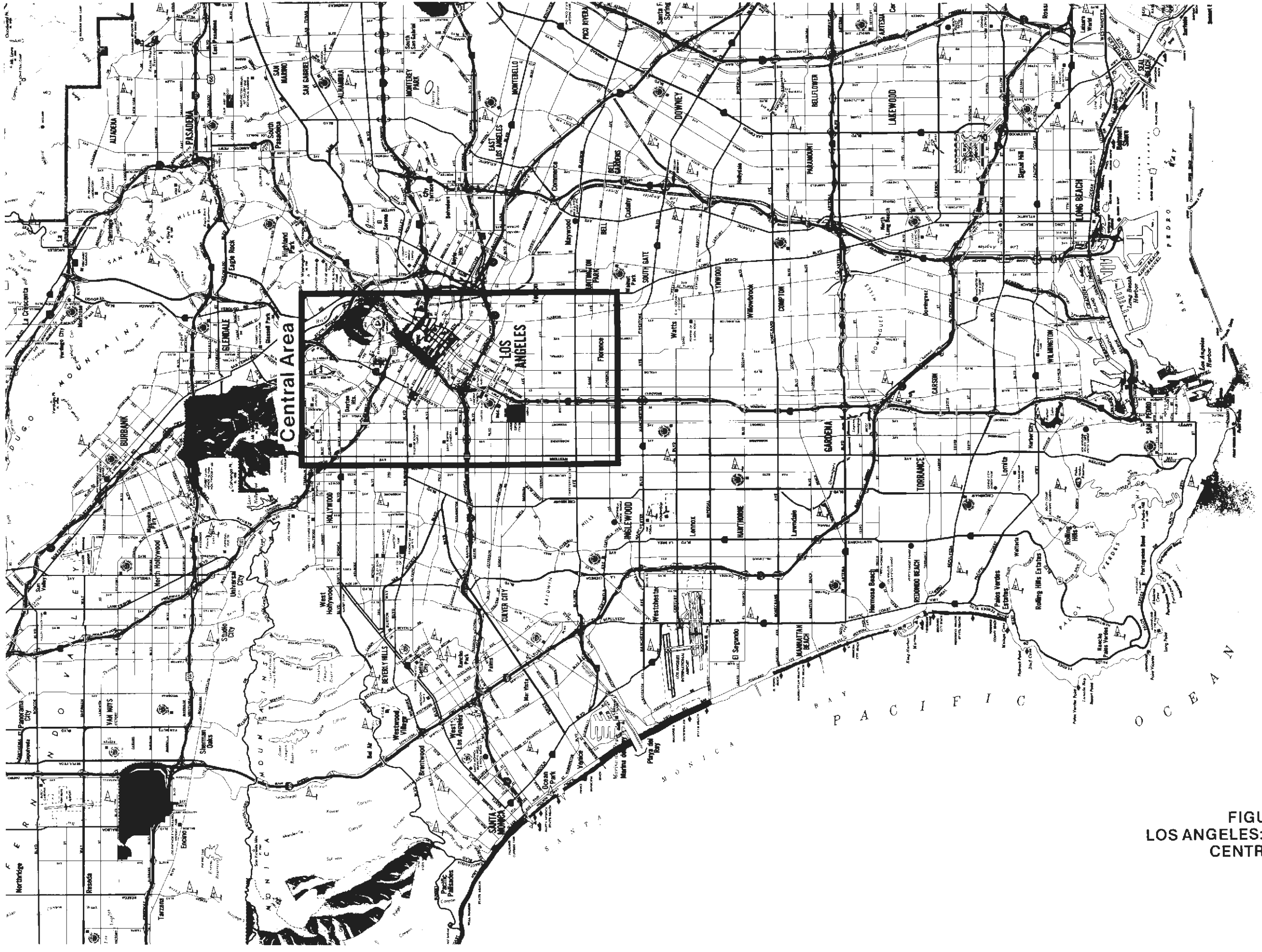

FIGURE 6
LOS ANGELES: WIDE AREA AND CENTRAL AREA

The error in reading the scale was estimated to be within 65 feet, which was small compared to most of the location errors. These longitudes and latitudes and the means of the TDs recorded at those points formed the data base used in the analysis.

However, more checking of the data base was required to be sure that it was as error-free as possible. To assure that the scales had been correctly read, another program plotted the points' locations using the measured longitudes and latitudes, and the plot was again overlaid on the map. The simplest flat earth model was then used with the measured TDs to generate a set of predicted longitudes and latitudes, the error was compared with the actual locations and was plotted as a vector. A similar technique used the flat earth model with the actual positions to compute TDs, with the differences from TDs measured at the point being plotted. Examining the printouts and plots for unusually large errors led to the discovery of some data entry errors, some points incorrectly located, and some points which obviously suffered cycle slip. After all such points were corrected, the two sets of "processed" data points were used to evaluate the algorithms.

After all "explainable" data base errors had been corrected, there remained points with relatively large errors which would only be attributed to the types of TD perturbations that it was hoped the various curve fits could improve. Coefficients were generated both with and without those points in the data base and were tested against the second sample. In general, better results were obtained when they were included (see Section 5.3).

To evaluate the "cost" side of the analysis, relative processing time and storage required were examined. Special purpose subroutines are available at the Metrek computer facility that allow one to determine how much CPU time has elapsed between calls to these subroutines. Judicious placement of calls allowed determination of only the time required for the position computation, excluding program initialization, extraneous read and write instructions, and the accumulation and statistical analysis of data. Core storage requirements were determined by compiling only the instructions that were required for the algorithm's computation. No attempt was made at optimization of either CPU time or storage, but the same general programming philosophy and techniques were used for all cases, so the relative comparisons should be valid. The time and storage requirements for the programs used to generate the various coefficients were not evaluated, as they are off-line programs that would be seldom used after the initial application. (For example, if sufficiently large seasonal variations made this desirable, or if experimentation with choice of sector boundaries were carried out.)

5. RESULTS

5.1 Accuracy

Table 2 summarizes the results of the tests performed. These data result from using the first sample to determine the best fit coefficients or conductivities, then using these constants with the second sample to simulate actual performance. In general, it can be seen that all methods gave approximately the same results: mean and 95th percentile errors corresponding to one and three blocks in the central area and three and five blocks over the wide area.

From previous discussion, it is obvious that more tests were performed than are shown. However, in general, the others give no better results and so are not included. For example, regressions from first to fifth order were run, but the second order gave results as good as, or better than, the others. (As was previously discussed, a second order regression would perfectly fit TDs that have no error--evidently the errors that do occur are not sufficiently regular to be better fit by a higher order regression.) Also, three forms of earth model were used in the theoretical method, and all had approximately the same accuracy. However, the flat earth model with extensive corrections required less computer time than the others, since it (and the precision earth model) required fewer iterations to converge than did the simplest flat earth model, and the precision earth model required more processing time per iteration. Although the numbers are not exactly the same for the various techniques, it is obvious, based on the size of the standard deviation compared to the differences in means or 95th percentiles, that there is no significant difference in accuracy between the various methods.

It is also obvious that the accuracy obtainable over the wide area is substantially degraded from that in the smaller central area. This is not to suggest that larger grid warpages occur outside the random route area, but rather perhaps that the variations over the larger area are sufficiently large and variable from area to area that one set of coefficients do not suffice. This seems to imply that subdividing the area into subareas, each with its own set of coefficients, should give better results. To test this hypothesis would require a density of data points over the wide area equivalent to that collected in the central area which was not available. It was found, however, that subdividing the points in the central into two geographically separated subareas each with its own set of regression coefficients, gave results inferior to treating the area as a whole. These results seem to define an approximate range for the size of area for which it is reasonable to compute separate coefficients; i.e., 400 square miles is too large, 30 square miles is much better, but 15 square miles is no better than 30 square miles.

TABLE 2 - ALGORITHM ACCURACIES

	Radial Error (Feet)					
	Central Area (30 Square Miles)			Wide Area (400 Square Miles)		
	Mean	Std. Dev.	95th %	Mean	Std. Dev.	95th %
Empirical (2nd Order Regression)	635	540	1,660	1,765	1,715	2,820
Theoretical (Flat Earth + Corrections)	640	555	1,710	1,540	1,530	2,800
Combination	620	660	1,845	1,525	1,725	2,835

Table 3 shows how well coefficients generated from the first sample fit the first sample, and can be viewed as a best-case accuracy. When comparing this to Table 2, it can be seen that the empirical and theoretical methods behave similarly. That is, the best-case results over the wide area are approximately 50 percent worse than for the central area (e.g., 800 feet mean error versus 555 feet, using the empirical method); when using the coefficients so generated to predict locations for the second sample, errors over the wide area are approximately 150 percent worse than for the central area (1,540 feet versus 640 feet). This seems to reinforce the previous hypothesis: the variations over the larger (wide) area cannot be fit as well as those in the central area, and the effect of the greater variation is magnified when the second sample, simulating actual use, is used.

Figure 7 illustrates the central area accuracy, which so far has been discussed in statistical terms. This figure is a location prediction plot generated by the combination method using the second sample. Such a plot allows one to visualize the effect that errors of the magnitude encountered would have in various applications. For example, such performance may be satisfactory for taxi service or delivery trucks, or for keeping track of the approximate locations of mobile supervisors and service vehicles, although it is obviously inadequate for determining bus schedule adherence.

In general, consistent bias is not apparent although there are a number of large errors in the southern part of the area, located near railroad tracks.

Figure 8 illustrates the method used to plot the time difference component errors. The actual TD pair is located at the actual map location, and the TD error components are defined as:

$$(TD_{computed} - TD_{measured})$$

If the measured time difference is larger than that computed (which can occur either as a result of the master signal arriving sooner than expected or the slave signal arriving later than expected), the error component is negative. Figure 8 shows the result of:

1. Measured TDA two units larger than computed, and measured TDB equal to that computed; and

2. Measured TDB two units larger than computed, and measured TDA equal to that computed.

TABLE 3 - ACCURACY OF FIT TO ORIGINAL SAMPLE

	Radial Error (Feet)					
	Central Area			Wide Area		
	Mean	Std. Dev.	95th %	Mean	Std. Dev.	95th %
Empirical	555	515	1,390	800	565	1,865
Theoretical	605	535	1,385	850	405	1,305
Combination	505	640	1,860	980	715	1,990

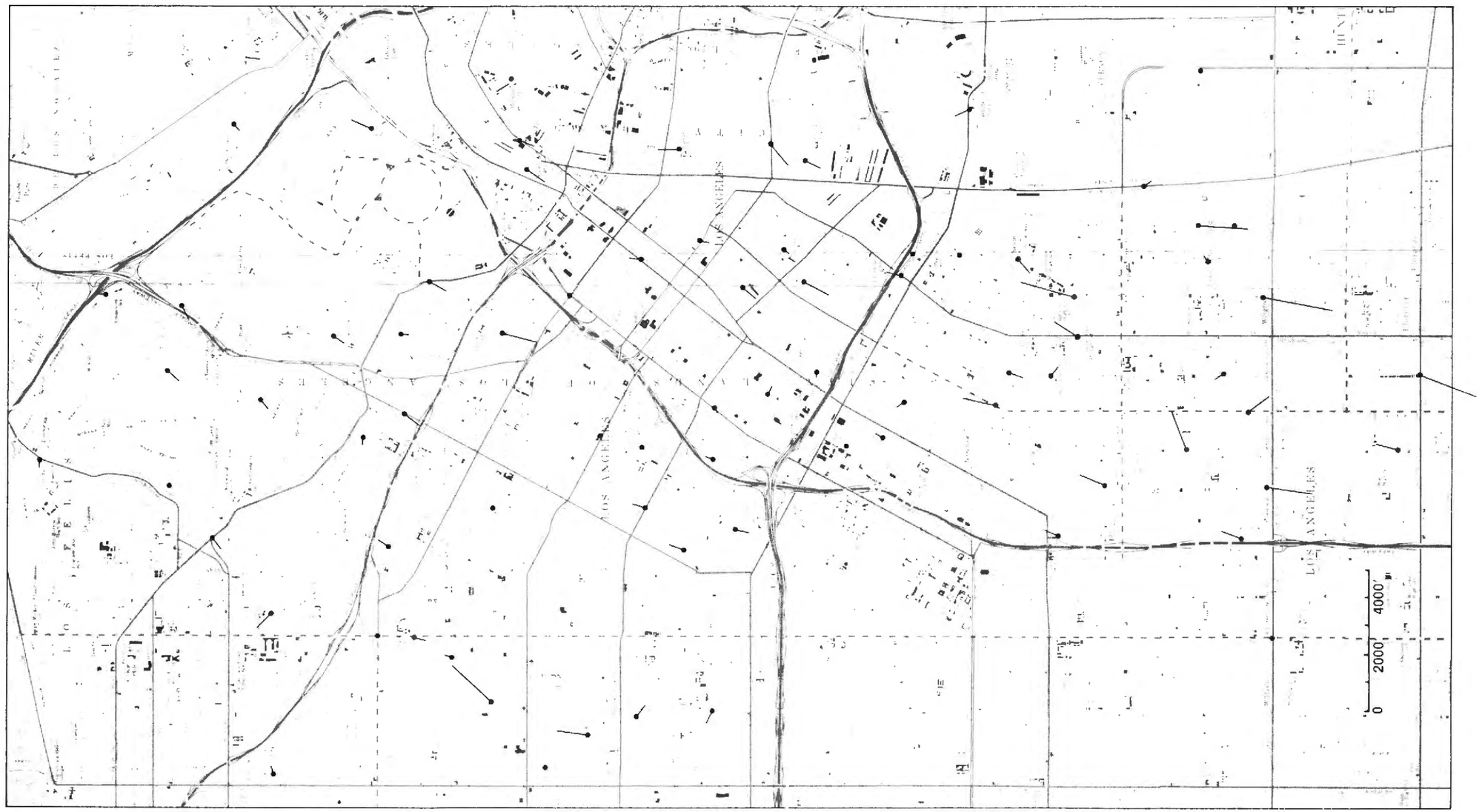

FIGURE 7
LOCATION ERROR PLOT

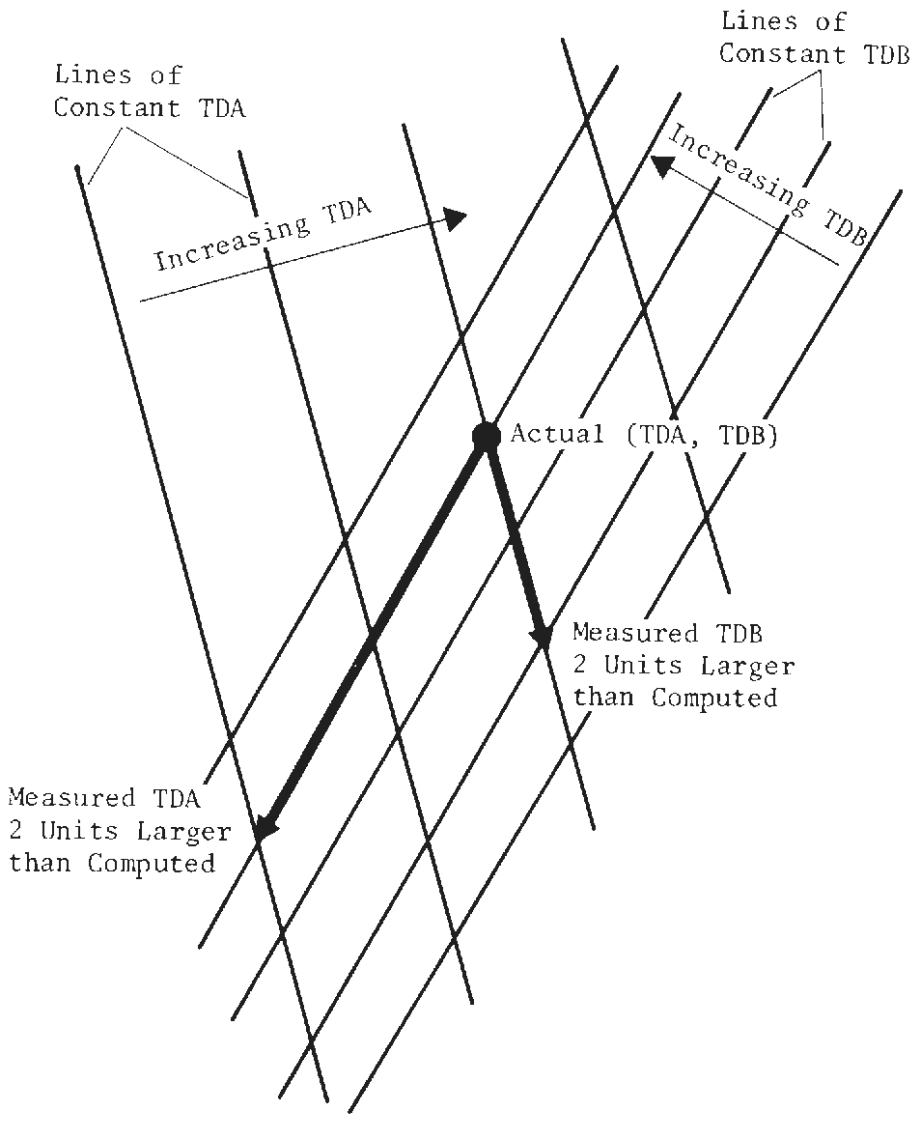

FIGURE 8
DECOMPOSITION OF TD ERRORS

Figure 9 shows the time difference errors corresponding to the location prediction errors in Figure 7. The large errors near the railroad tracks, previously noted, are the result of nearly equal TDA and TDB errors. Both TD components are larger than expected, indicating that the master signal arrives sooner than expected or that both slave signals arrive later than computed. (The TD scales were chosen to correspond approximately to the distance errors plotted in Figure 7. The magnitude and direction of the TD error components do not form enough of a consistent pattern in any geographic area to suggest subdivision into smaller sectors.

It was previously noted that the radial error statistics for the three methods are similar. In fact, as shown by Figure 10, a reduced overlay of predicted versus actual location for all three techniques, the actual locations predicted by each method are also similar. (Only the overlay is shown to enable one better to distinguish between the various vectors.) Comparing Tables 4 and 2 also indicates that the predicted locations are closer to each other than they are to the actual point; with the mean radial differences being approximately half the mean radial error, and the 95th percentile differences being one-half to one-third of the 95th percentile radial error.

5.2 Computer Requirements

Core required by the computational parts of the Fortran program is approximately 30 kilobytes for each method, while the times required to compute the location of one data point are:

Empirical	15 ms
Theoretical:	
Flat Earth & Mid-Latitude Correction	85 ms
Flat Earth & Extensive Corrections	65 ms
Precision Earth	105 ms
Combination	125 ms

That is, the empirical regression method is four times faster than the next method, the theoretical flat earth with extensive corrections. In turn this is faster than the simplest flat earth model, since fewer iterations are required for convergence. Further range and bearing accuracy improvement provided by the precision earth model did not further decrease the number of iterations required, and as the precision earth model is also used in the combination method, there is no offsetting of the increased time required by their more complex calculations.

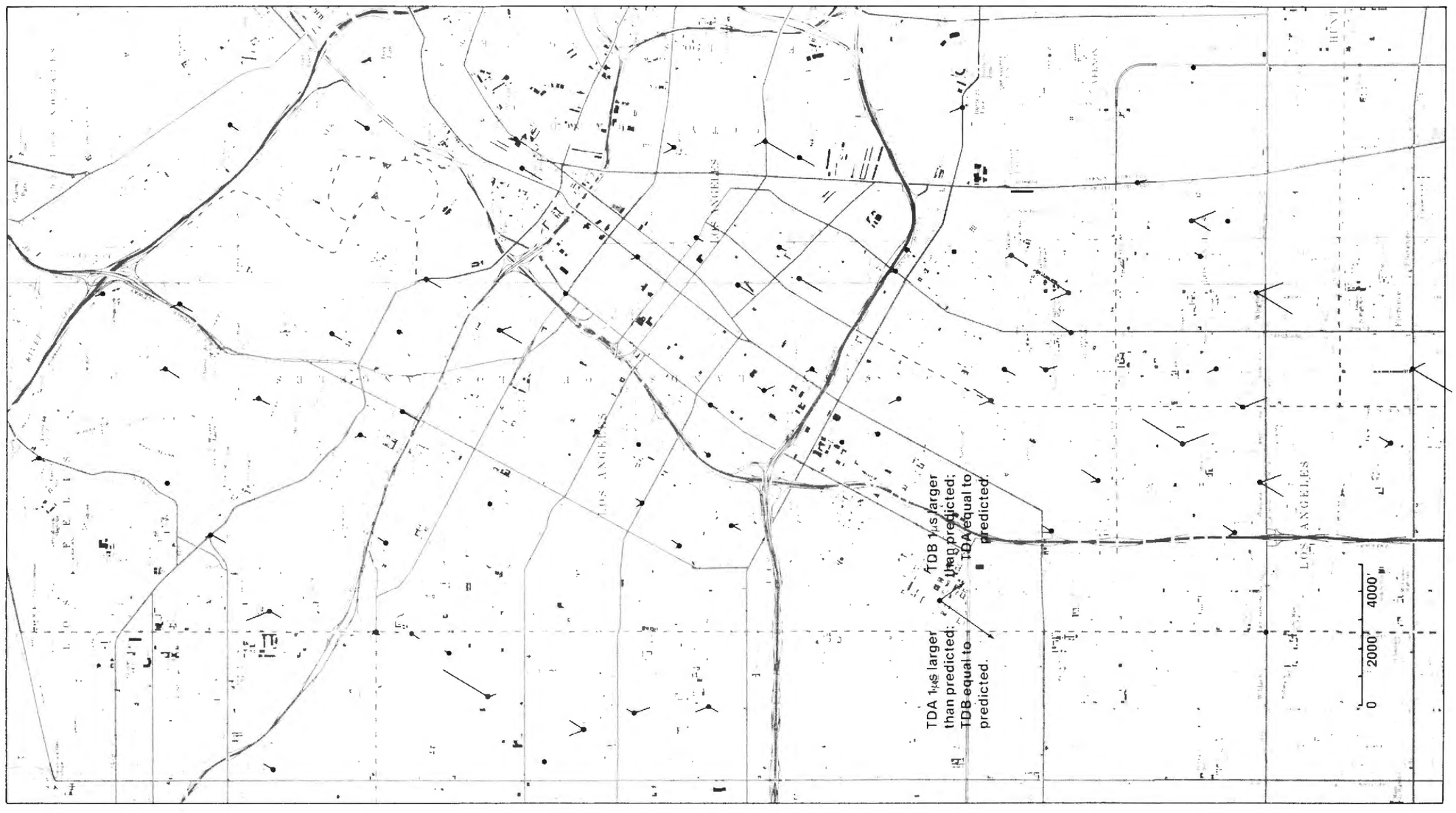

FIGURE 9
TD ERROR PLOT

TABLE 4 - RADIAL DIFFERENCES IN LOCATION PREDICTIONS

	Mean (Feet)	Standard Deviation (Feet)	95th Percentile (Feet)
Empirical vs. Theoretical	335	190	660
Theoretical vs. Combination	270	175	515
Empirical vs. Combination	370	270	950

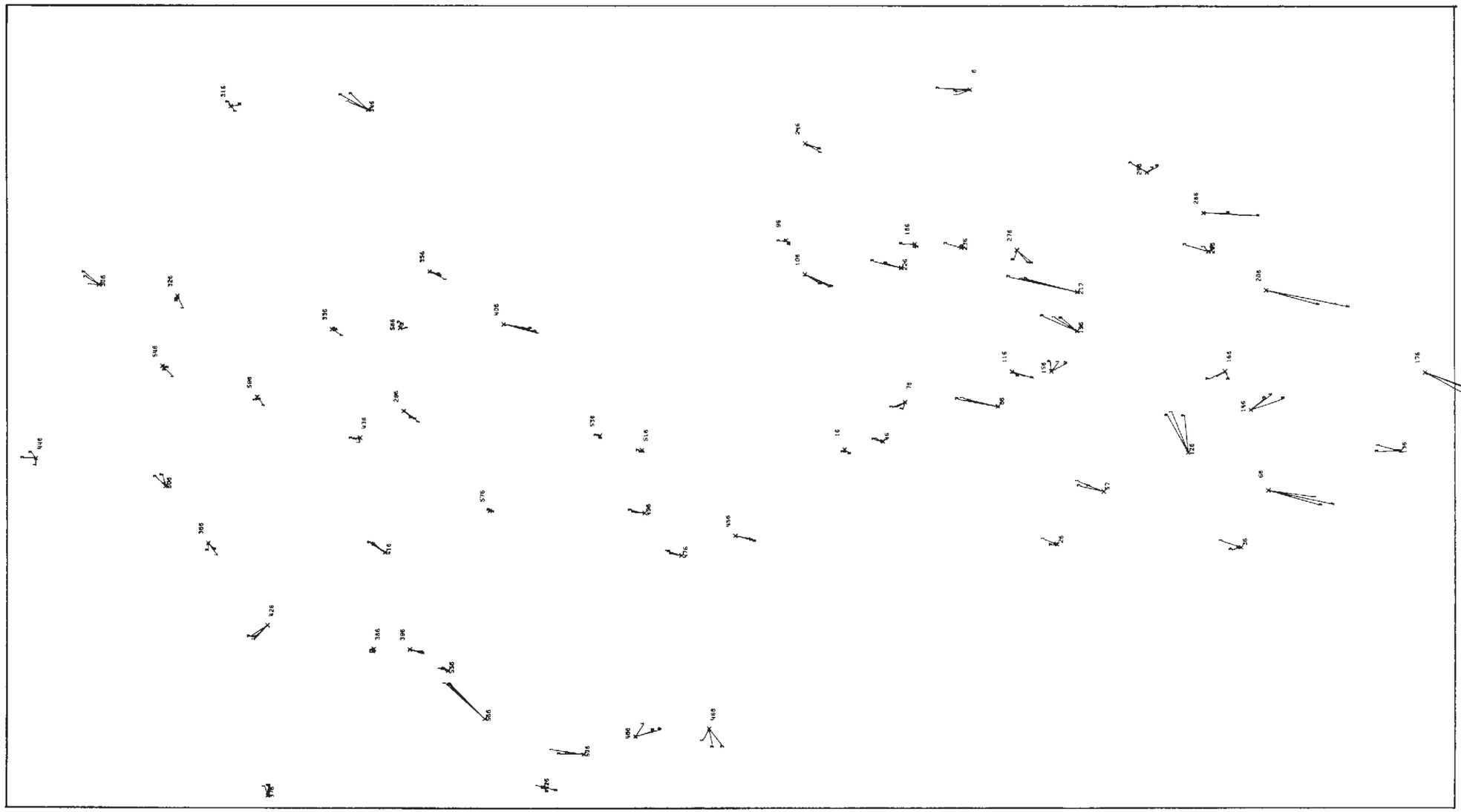

FIGURE 10
COMPARISON OF LOCATION ERROR
OF ALL THREE TECHNIQUES

5.3 Other Analyses

As all of the techniques, as used here, require that calibration points be chosen to determine the best set of coefficients to represent the given area, the question of how to choose which calibration points to use is of interest. One method that has been suggested is to use points that exhibit small TD variability with repeated measurements, the theory being that a more stable measurement is also more accurate. Figure 11 plots the rms value of the range of TDA and TDB for each point in the first sample (i.e., the difference between the largest and smallest of the three TD pairs measured at each point) versus the resultant accuracy when those points were used with the empirical method. It can be seen that for the majority of the points, a given accuracy is as likely to occur for a point where 160 ns variability occurred as for a point exhibiting 40 ns variability. Although those points with the largest errors do seem to follow a linear (or quadratic) relationship with TD variability, this does not help in choosing a priori which points to use in determining the best coefficients.

As previously noted, it was found somewhat better to use all "valid" data points in the computation (that is, including those that result in relatively large errors when they are used with the coefficients generated). "Tail" errors, e.g., 95th percentile of the second sample, were reduced by 300 feet when all valid points in the first sample were included, as compared with excluding those with errors over 1,000 feet.

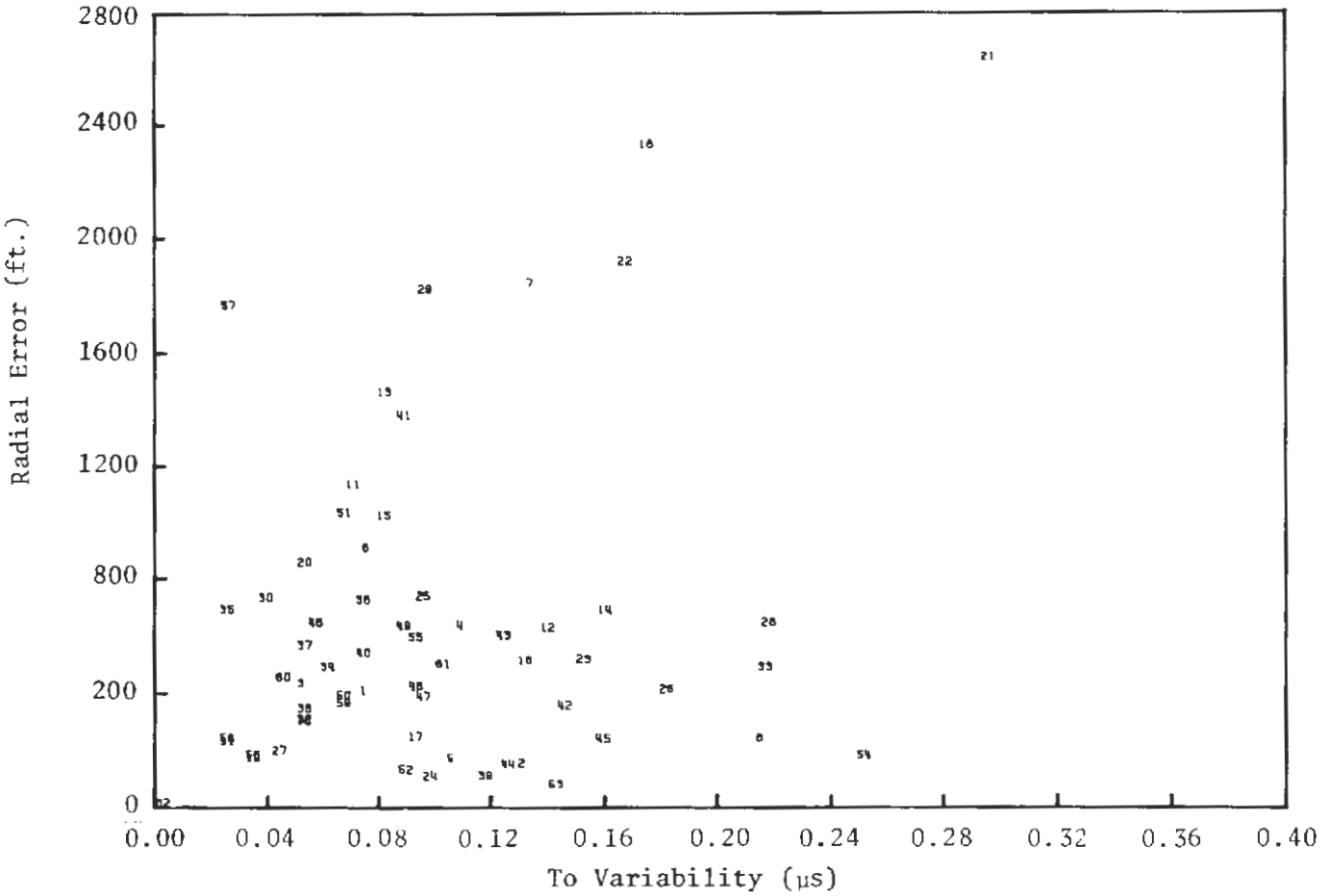

FIGURE 11
TD VARIABILITY VS ACCURACY

6. CONCLUSIONS

Based on the analysis, none of the techniques would be sufficiently accurate to meet the stringent random route accuracy requirements of the AVM demonstration program. That is, Loran alone would not be adequate to replace the signposts for this function. To improve upon this accuracy, the hybrid technique presently being developed for the Los Angeles demonstration uses on-board Loran processing, differential odometer data and Kalman filtering. Further tests will determine the extent of the accuracy improvement.

The accuracy attainable using only Loran, however, may be adequate for many applications, as can be seen from the plots. As all of the algorithms gave approximately the same results, the second order regression technique is the one to choose for use in any reasonably sized area, e.g., on a metropolitan area scale, as it is the simplest and fastest executing. It can be performed on-board a vehicle using a microprocessor, even including coefficients for multiple sectors. For application in larger areas requiring many sectors, e.g., on a statewide scale, the flat earth method would probably give more satisfactory results and can also be implemented aboard a vehicle.

REFERENCES

[1] Blood, B.E. and B.W.A. Kliem, "Experiments on Four Different Techniques for Automatically Locating Vehicles, A Summary of Results," DOT/TSC, UMTA-MA-06-0041-77-2, Cambridge, Massachusetts, June 1977.

[2] Ludwick, J.S., Jr., "Analysis of Data from an Automatic Vehicle Monitoring Test," The MITRE Corporation, Metrek Division, MTR-7702, McLean, Virginia, January 1978.

[3] Vincent, W.R. and G. Sage, "Loran-C RFI and Noise; Los Angeles, California," Systems Control Incorporated, Report No: 6893/6894-0279, Palo Alto, California, February 1979.

[4] Teledyne Systems Company, "LAVM Location Subsystem Test Plan, Data Analysis Plan, Volume 1," Northridge, California, 1976.

[5] Howard, J., "LORAN Prediction and Coordinate Conversion," The MITRE Corporation, WP-21504, Rev. 1, Bedford, Massachusetts, January 1978.

[6] Lear Siegler, Incorporated, "AN/ARN-101 Computer Program Development Specification, RF-4C," CB1001-004, Contract F19628-76-C-0024, 1976.

APPENDIX A - EXAMPLE OF LEAST SQUARE DERIVATION

The example given is for the derivation of least squares second order regression coefficients (c_{ij}). We want to minimize:

$$SS_X = \sum_{i=1}^{n} (X_i - \hat{X}_i)^2$$

Where:

X_i is the actual X position of the $i^{\underline{th}}$ calibration point,

$\hat{X}_i$ is the predicted X position of the $i^{\underline{th}}$ calibration point,

N is the number of calibration points.

Assume X_i is to be determined as a second order function of $(TDA_i - TDAR)$ and $(TDB_i - TDBR)$, abbreviated here as A_i and B_i:

$$SS_X = \Sigma [X_i - (XR + C_{11}A_i + C_{12}B_i + C_{13}A_i^2 + C_{14}A_iB_i + C_{15}B_i^2)]^2$$

$$\frac{\partial SS_X}{C_{11}} = \Sigma (2) [x_i - (XR + C_{11}A_i + C_{12}B_i + C_{13}A_i^2 + C_{14}A_iB_i + C_{15}B_i^2)][-A_i] = 0$$

$$\frac{\partial SS_X}{\partial C_{12}} = \Sigma (2) [x_i - (XR + C_{11}A_i + C_{12}B_i + C_{13}A_i^2 + C_{14}A_iB_i + C_{15}B_i^2)][-B_i] = 0$$

etc.

or

$$C_{11}\Sigma A_i^2 + C_{12}\Sigma A_iB_i + C_{13}\Sigma A_i^3 + C_{14}\Sigma A_i^2B_i + C_{15}\Sigma A_iB_i^2 = \Sigma X_iA_i - XR\Sigma A_i$$

$$C_{11}\Sigma A_iB_i + C_{12}\Sigma B_i^2 + C_{13}\Sigma A_i^2B_i + C_{14}\Sigma A_iB_i^2 + C_{15}\Sigma B_i^3 = \Sigma X_iB_i - XR\Sigma B_i$$

This system of equations can be represented as a matrix equation:

$$MC = N$$

Where:

$$M = \begin{bmatrix} \Sigma A_i^2 & \Sigma A_i B_i & \Sigma A_i^3 & \Sigma A_i^2 B_i & \Sigma A_i B_i^2 \\ \Sigma A_i B_i & \Sigma B_i^2 & \Sigma A_i^2 B_i & \Sigma A_i B_i^2 & \Sigma B_i^3 \\ & & \vdots & & \end{bmatrix}$$

$$C = \begin{bmatrix} C_{11} \\ C_{12} \\ C_{13} \\ C_{14} \\ C_{15} \end{bmatrix}$$

$$N = \begin{bmatrix} \Sigma X_i A_i - XR\Sigma A_i \\ \Sigma X_i B_i - XR\Sigma B_i \\ \vdots \end{bmatrix}$$

Therefore, if M is non-singular, $C=M^{-1}N$. To compute $[C_{21}, C_{22}, C_{23}, C_{24}, C_{25}]^T$ the same matrix M results, therefore, the inverse previously computed can be used to multiply a vector formed by replacing, in N, X_i with Y_i, and XR with YR. A similar approach holds for higher order regression equations.

APPENDIX B - EARTH MODELS FOR THEORETICAL METHOD

The three earth models used with the theoretical technique are:

- o Flat earth with mid-latitude correction
- o Flat earth with extensive corrections
- o Precision earth.

They are used to determine the range and bearing between two known lat./long. pairs on the surface of the earth. The following definitions are common to all methods:

ϕ_s, ϕ_r - geodetic latitudes (degrees) of transmitter s and reference position

λ_s, λ_r - geodetic longitudes (degrees) of transmitter s reference position

ρ_s - range (feet) between transmitter s and reference position

θ_s - angle (degrees) between transmitter s and reference position

B.1 Flat Earth with Mid-Latitude Correction

$C_{AVE} = (\cos \phi_s + \cos \phi_r)/2$

$R_E = R_e$ = equatorial radius= 20,925,873 feet

$R_N = R_e(1-f)$ where

f= flattening= 1/295

$R_X = (\lambda_r - \lambda_s) R_E C_{AVE}$ DR where

DR= degree to radian conversion factor= $\Pi/180$

$R_Y = (\phi_r - \phi_s) R_N$ DR

θ_s = Arctan (R_Y/R_X)

$\rho_s = (R_X^2 + R_Y^2)^{1/2}$

B.2 Flat Earth with Extensive Corrections

$R_E = Re\ (1+f \sin^2 \phi_r)$

$R_N = Re\ (1-2f+3f \sin^2 \phi_r)$

R_X, R_Y, ρ_s and ϕ_s are then computed as before.

$\theta_c = (\rho_s \sin \phi_s)/(\pi R_e \quad DR \cos \phi_r)$

$\theta_s = \theta_s - \theta_c$

That is, an additional correction factor is subtracted from the bearing previously computed.

B.3 Precision Earth

$\beta_r = \text{Arctan}\ ((1-f) \tan \phi_r)$

$\beta_s = \text{Arctan}\ ((1-f) \tan \phi_s)$

$C_{1s} = \cos \beta_s \sin(\lambda_s - \lambda_r)$

$C_{2s} = \cos \beta_r \sin \beta_s - \sin \beta_r \cos \beta_s \cos (\lambda_s - \lambda_r)$

$C_{3s} = \sin \beta_r \sin \beta_s + \cos \beta_r \cos \beta_s \cos (\lambda_s - \lambda_r)$

$\psi_s = \text{Arctan}\ (C_{1s}/C_{2s})$

$\theta_s = \text{Arctan}\ ((C_{2s} \cos \psi_s + C_{1s} \sin \psi_s)/C_{3s})$

$\rho_s = K_1\theta_s + K_2(\theta_s \sin^2 \psi_s \cos^2 \beta_r) + K_3 \tan\theta_s (\sin^2 \psi_s \cos^2 \beta_r - \cos^2 \beta_s)$

Where the K's are spheroid constants:

$K_1 = 20,890,417.498275$

$K_2 = 35,442.999770$

$K_3 = 35,459.227609$

$K_4 = 294.978698$